Granulosa Cell-Expressed BMPR1A and BMPR1B Have Unique Functions in Regulating Fertility but Act Redundantly to Suppress Ovarian Tumor Development

Mark A. Edson, Roopa L. Nalam, Caterina Clementi, Heather L. Franco, Francesco J. DeMayo, Karen M. Lyons, Stephanie A. Pangas, and Martin M. Matzuk

Departments of Pathology (M.A.E., C.C., R.L.N., S.A.P., M.M.M.), Molecular and Cellular Biology (M.A.E., R.L.N., H.L.F., F.J.D., M.M.M.), and Molecular and Human Genetics (M.M.M.), and Program in Developmental Biology (C.C., F.J.D., M.M.M.), Baylor College of Medicine, Houston, Texas 77030; and Departments of Orthopaedic Surgery; Biological Chemistry; and Molecular, Cell, and Developmental Biology (K.M.L.), University of California Los Angeles, Los Angeles, California 90095

Bone morphogenetic proteins (BMPs) have diverse roles in development and reproduction. Although several BMPs are produced by oocytes, thecal cells, and granulosa cells of developing follicles, the *in vivo* functions of most of these ligands are unknown. BMP signals are transduced by multiple type I and type II TGFβ family receptors, and of the type I receptors, BMP receptor 1A (BMPR1A) and BMP receptor 1B (BMPR1B) are known to be expressed in rodent granulosa cells. Female mice homozygous null for *Bmpr1b* are sterile due to compromised cumulus expansion, but the function of BMPR1A in the ovary is unknown. To further decipher a role for BMP signaling in mouse granulosa cells, we deleted *Bmpr1a* in the granulosa cells of the ovary and found *Bmpr1a* conditional knockout females to be subfertile with reduced spontaneous ovulation. To explore the redundant functions of BMP receptor signaling in the ovary, we generated *Bmpr1a Bmpr1b* double-mutant mice, which developed granulosa cell tumors that have evidence of increased TGFβ and hedgehog signaling. Thus, similar to SMAD1 and SMAD5, which have redundant roles in suppressing granulosa cell tumor development in mice, two type I BMP receptors, BMPR1A and BMPR1B, function together to prevent ovarian tumorigenesis. These studies support a role for a functional BMP signaling axis as a tumor suppressor pathway in the ovary, with BMPR1A and BMPR1B acting downstream of BMP ligands and upstream of BMP receptor SMADs. **(*Molecular Endocrinology* 24: 1251–1266, 2010)**

Ligands of the TGFβ superfamily have diverse roles in developmental, physiological, and pathological processes (1, 2). Members of this family, which include inhibins, activins, growth and differentiation factors (GDFs), myostatin, and bone morphogenetic proteins (BMPs), signal through an oligomeric complex of type I and type II TGFβ serine/threonine kinase receptors. Ligand-induced phosphorylation of type I receptors, also called activin receptor (ACVR)-like kinases (ALKs), by a type II receptor results in the phosphorylation and activation of receptor-regulated SMAD proteins (R-SMADs) that associate with the common SMAD4 protein to regulate gene expression (1, 3). The BMPs are the largest subfamily of TGFβ-related ligands, and the specificity of their signaling is partially determined by distinct ligand-receptor interactions. Three type II receptors are capable

ISSN Print 0888-8809 ISSN Online 1944-9917
Printed in U.S.A.

doi: 10.1210/me.2009-0461 Received November 6, 2009. Accepted March 1, 2010.
First Published Online April 2, 2010

Abbreviations: ACVR, Activin receptor; ALK, ACVR-like kinase; AMH, anti-Müllerian hormone; BMP, bone morphogenetic protein; BMPR2, type II BMP receptor; cKO, conditional knockout; COC, cumulus-oocyte complex; dKO, double knockout; GDF, growth and differentiation factor; hCG, human chorionic gonadotropin; MOF, multi-oocyte follicle; PMSG, pregnant mare serum gonadotropin; PTCH, patched; QPCR, quantitative PCR; R-SMAD, receptor-regulated SMAD protein; SMO, smoothened; WT, wild type; ZPR, zona pellucida remnant.

of binding BMPs, including the prototypical type II BMP receptor (BMPR2), and the type IIA and IIB ACVRs (ACVR2A and ACVR2B), which also bind activins and myostatin (4). There are also three type I BMP receptors, which include the type IA and IB BMP receptors, BMPR1a (also known as ALK3) and BMPR1B (also known as ALK6), and the type I ACVR, ACVR1 (also known as ALK2) (4, 5). The R-SMADS activated by these BMP receptors include SMAD1, SMAD5, and SMAD8 (referred to as BR-SMADs). In contrast to BMPs, TGFβs, activins, GDF9, nodal, and myostatin generally signal through SMAD2 or SMAD3 (referred to as AR-SMADs) pathways (1, 3).

Within the mammalian ovary, communication between the oocyte, granulosa cells, and thecal cells regulates follicular development. Genetic studies at several levels of the TGFβ signaling pathway have identified crucial functions of ligands, receptors, and intracellular SMADs during normal reproductive processes and in the prevention of cancer (1, 2, 7). Interestingly, distinct ovarian phenotypes are caused by conditional ablation [referred to as conditional knockout (cKO)] of either of the R-SMAD signaling pathways or the common SMAD4 (8–10). *Smad4* cKO mice are subfertile with follicles that undergo premature luteinization as well as defects in cumulus expansion (9). At the level of the R-SMADs, individual deletion of SMAD2 or SMAD3 in the ovary does not significantly affect fertility or folliculogenesis (8). In contrast, mice deficient in both SMAD2 and SMAD3 in granulosa cells have severe fertility defects and share some features with *Smad4* cKO mice, such as impaired cumulus expansion, although luteinization defects are not as prominent and serum progesterone is not elevated (8). SMAD1 and SMAD5 are also functionally redundant in the ovary. Mice deficient in either SMAD1 or SMAD5 in the ovary do not have fertility defects, but *Smad1 Smad5* double-cKO (herein referred to as *Smad1 Smad5* cKO) females are subfertile and develop metastatic granulosa cell tumors, suggesting that SMAD1/5 signaling in granulosa cells acts as a tumor suppressor pathway, potentially by antagonizing SMAD2/3 signaling (10, 11).

Because of the large number of BMPs produced by multiple cell types in the ovary (12, 13) and the embryonic or perinatal lethality of most BMP knockout mice, studying the individual and redundant impact of several BMPs concurrently on granulosa cells is technically challenging. An alternative approach is to study BMP signaling by genetic ablation of individual receptors. Based on *in situ* hybridization studies in the rodent ovary, both *Bmpr1a* and *Bmpr1b* are expressed in the granulosa cells of growing follicles (12). *Bmpr1b*-null mice are sterile because of impaired cumulus expansion (14); however, the development of granulosa cell tumors in these mice has not been evaluated. A role for BMPR1A in ovarian physiology has not been determined, and although BMPR1A and BMPR1B have been shown to have overlapping functions in other biological systems (15, 16), the degree of redundancy in the ovary is unknown. Moreover, it is likely that each receptor has unique functions, because BMPR1A does not compensate for BMPR1B in cumulus expansion and *in vitro* evidence suggests oocyte-secreted BMP15 preferentially binds to BMPR1B over BMPR1A (17, 18). To investigate the individual and redundant roles of BMPR1A and BMPR1B as mediators of BMP signaling in ovarian granulosa cells and to circumvent the embryonic lethality of *Bmpr1a*-null mutations (19), we used the *Cre-loxP* system to generate tissue-specific *Bmpr1a* cKO mice as well as *Bmpr1a* cKO *Bmpr1b*$^{-/-}$ double-knockout (dKO) mice. Although *Bmpr1a* cKO females have fertility defects distinct from *Bmpr1b*-null females, we found that BMPs signal redundantly through BMPR1A and BMPR1B to suppress the development of granulosa cell tumors. Molecularly, the tumors in *Bmpr1a Bmpr1b* dKO females exhibit elevated levels of TGFβs and TGFβ target genes as well as up-regulation of mediators of hedgehog signaling. Therefore, we hypothesize that part of the function of these type I receptors in preventing tumorigenesis may be by modulating multiple intraovarian signaling pathways. Our results strongly support an *in vivo* role for BMP signaling pathways in tumor suppression in the ovary.

Results

Generation of *Bmpr1a* cKO and *Bmpr1a cKO Bmpr1b*$^{-/-}$ double-mutant mice

To determine the role of BMPR1A in the ovary and to overcome the early embryonic lethality of complete *Bmpr1a* ablation (19), we generated *Bmpr1a* cKO mice using Cre recombinase under the control of the *Amhr2* promoter (20). Recombination of the *Bmpr1a* conditional allele completely inactivates BMPR1A function (21). Using the *Rosa26* reporter mouse (22), *Amhr2-Cre* expression in the postnatal ovary has been detected predominantly in the granulosa cells of growing follicles (23, 24); however, some studies have reported expression of *Amhr2-Cre* in the ovarian surface epithelium (25) as well as low levels of expression in thecal cells (24). To achieve maximal reduction of BMPR1A, *Bmpr1a*$^{+/-}$ *Amhr2*$^{cre/+}$ mice were crossed to *Bmpr1a*$^{Flox/Flox}$ mice to generate *Bmpr1a*$^{Flox/-}$ *Amhr2*$^{cre/+}$ experimental mice (designated throughout as *Bmpr1a* cKO mice), *Bmpr1a*$^{Flox/-}$ (designated as control), and *Bmpr1a*$^{Flox/+}$ mice. We assessed recombination of the *Bmpr1a* floxed allele in granulosa

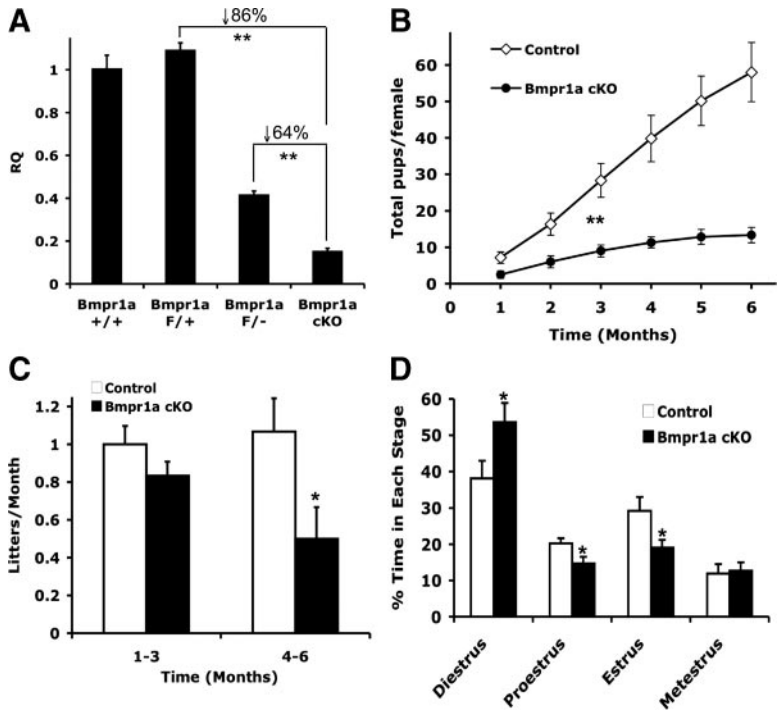

FIG. 1. Fertility and estrous cycle analysis in control and *Bmpr1a* cKO females. A, Relative *Bmpr1a* mRNA in granulosa cells of *Bmpr1a*$^{+/+}$, *Bmpr1a*$^{Flox/+}$, *Bmpr1a*$^{Flox/-}$, and *Bmpr1a*$^{Flox/-}$ *Amhr2*$^{cre/+}$ (*Bmpr1a* cKO) mice (RQ, relative quantity of transcript); B, average number of pups produced by control and *Bmpr1a* cKO females over the course of 6 months of breeding (n = 6 per genotype); C, in addition to smaller litters (see text), *Bmpr1a* cKO females had fewer litters per month, and this was more pronounced in the last half of the breeding period; D, estrous cycle monitoring of 7-month-old mice over the course of 1 month demonstrated *Bmpr1a* cKO females (n = 9) spent significantly more time in diestrus and less time in proestrus and estrus compared with control females (n = 6). *, $P < 0.05$; **, $P < 0.01$ (Student's *t* test).

cells by real-time quantitative PCR (QPCR) analysis of cDNA prepared from *Bmpr1a*$^{Flox/+}$, *Bmpr1a*$^{Flox/-}$, and *Bmpr1a* cKO granulosa cells obtained from hormonally primed mice. In *Bmpr1a* cKO granulosa cells, *Bmpr1a* mRNA levels are 86% lower than in *Bmpr1a*$^{Flox/+}$granulosa cells and 64% lower than *Bmpr1a*$^{Flox/-}$ control mice (Fig. 1A). In addition, to confirm that *Bmpr1a* expression is not affected by the presence of loxP sites, we compared transcript levels in *Bmpr1a*$^{+/+}$ and *Bmpr1a*$^{Flox/+}$ granulosa cells and confirmed that *Bmpr1a* expression is not statistically different (Fig. 1A). Therefore, in the remaining studies, *Bmpr1a*$^{Flox/+}$ mice are designated as wild type (WT).

Bmpr1a cKO female mice are subfertile

BMPR1B has previously been shown to be required for female fertility (14). To assess a role for BMPR1A in female fertility, 6-wk-old *Bmpr1a* cKO and control mice were bred to WT males over the course of 6 months. During this time period, *Bmpr1a* cKO mice exhibited a significant reduction in fertility and fecundity. The control females demonstrated a cumulative increase in pups and produced an average of 58 ± 8.1 pups over 6 months of breeding with an average litter size of 9.0 ± 0.8 pups per litter. In contrast, *Bmpr1a* cKO females had only 3.4 ± 0.5 pups per litter ($P < 0.01$), and the cumulative number of offspring generated was significantly reduced, with only 13.3 ± 2.1 pups born per female at the end of the 6-month breeding period (Fig. 1B). *Bmpr1a* cKO females also had fewer litters per month (0.7 ± 0.1 *vs.* 0.9 ± 0.7 for control, $P < 0.05$). After only 4 months of breeding, half of the *Bmpr1a* cKO female mice were infertile, and this was further evident by 6 months of breeding whereby the majority of *Bmpr1a* cKO females demonstrated infertility. In addition, similar to the littermate control females used in the fertility studies, *Bmpr1a*$^{+/-}$ *Amhr2*$^{cre/+}$ females that were used in crosses to generate *Bmpr1a* cKO mice did not exhibit fertility defects over the course of 8–12 months of breeding (data not shown).

Consistent with the decreased fertility and fecundity, which was more pronounced in the latter half of the breeding period (Fig. 1C), *Bmpr1a* cKO mice exhibited a prolonged diestrous phase beginning at approximately 7 months of age (Fig. 1D). In contrast, there was no difference in the length or periodicity of estrous cycles when the same group of females was monitored beginning at 6–8 wk of age (data not shown), a time at which fecundity was not impaired in *Bmpr1a* cKO females.

The primary cause of sterility in *Bmpr1b*-null females is a failure of fertilization *in vivo*, secondary to defects in cumulus expansion (14). To determine whether the subfertility phenotype in *Bmpr1a* cKO females could be due to impaired cumulus expansion, cumulus-oocyte complexes (COCs) were collected from the ampulla of immature control and mutant mice subjected to a superovulation regimen of pregnant mare serum gonadotropin (PMSG) followed by human chorionic gonadotropin (hCG). Although the mean number of COCs recovered from *Bmpr1a* cKO mice was lower than from controls, the differences were not significant (34.9 ± 7.4, n =10, and 48.3 ± 6.1, n = 7, respectively; $P = 0.4$), and in contrast to the failure of cumulus expansion in COCs from *Bmpr1b*-null mice, COCs from *Bmpr1a* cKO mice underwent normal expansion *in vivo* (Fig. 2, A and B). Despite a statistically normal ovulatory response of im-

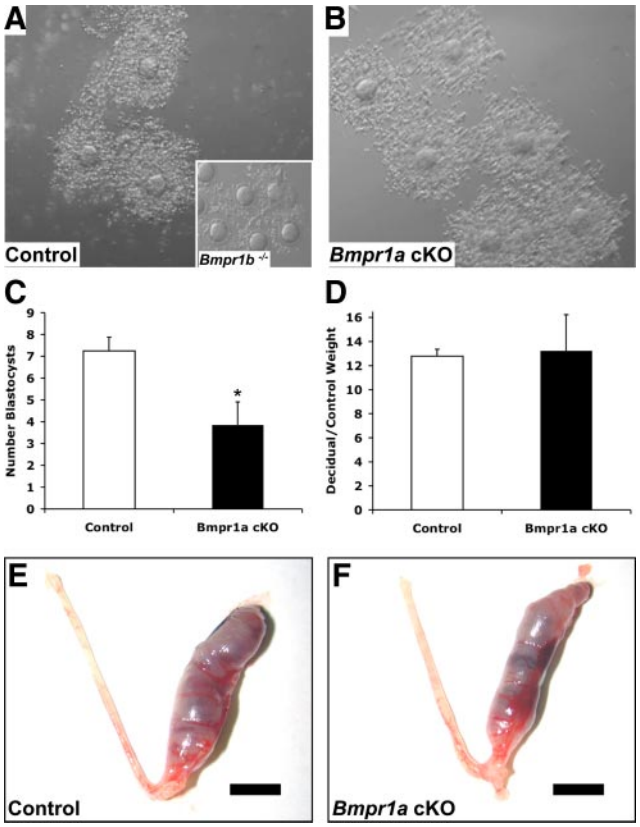

FIG. 2. Cumulus expansion and uterine decidual response are intact in *Bmpr1a* cKO mice. Immature female mice were superovulated, and COCs were obtained from the ampulla of the oviduct 16–18 h after hCG. A, Normal cumulus expansion in a control female, in contrast to impaired expansion and to poor adherence of cumulus cells around the oocyte in *Bmpr1b*$^{-/-}$ (*inset*); B, cumulus expansion in *Bmpr1a* cKO females is intact; C, *Bmpr1a* cKO mice have a decrease in spontaneous ovulation, as determined by the number of blastocysts recovered from the uterus 3.5 d after mating with WT males (*, $P < 0.05$); D–F, there is no difference in the response to artificial induction of decidualization in control (E) *vs.* *Bmpr1a* cKO mice (F). *Scale bar* (E and F), 5 mm.

mature *Bmpr1a* cKO females after exogenous gonadotropins, *Bmpr1a* cKO females spontaneously ovulated fewer COCs when subjected to natural matings, as determined by the number of blastocysts recovered from the uteri of control and mutant females (7.25 ± 0.63 *vs.* 3.86 ± 1.06, $P < 0.05$; Fig. 2C).

Recombination also occurs in the uterus of *Amhr2-Cre* mice, specifically in the smooth muscle cells of the uterine myometrium and weakly in the endometrial stromal cells (26), indicating that a uterine defect could possibly contribute to the observed subfertility. Previously, BMP2 signaling was demonstrated to be essential for the proliferation and differentiation of the uterine stroma in a process known as decidualization (27). In the rat uterus, *Bmpr1a* is widely expressed, and within the myometrium, transcripts are detected in the circular and longitudinal smooth muscle layers (28). Because of a decrease in spontaneous ovulation in *Bmpr1a* cKO females and to eliminate confounding hypothalamic-pituitary-ovarian factors, we evaluated decidualization by inducing an artificial decidual reaction in ovariectomized females (29). Induction of decidualization occurred in both control and *Bmpr1a* cKO mice, and decidualized uteri from both groups showed a similar increase in size *vs.* the unstimulated control uterine horns (Fig. 2, D–F). These findings suggest that reduced spontaneous ovulation, but not defects in uterine decidualization, contributes to the subfertility of the *Bmpr1a* cKO mice.

Bmpr1a cKO and *Bmpr1a Bmpr1b* dKO mice have disrupted follicular development

To assess potential ovarian defects that might contribute to the subfertility and decreased spontaneous ovulation *Bmpr1a* cKO females, we compared ovaries from 3-month-old control and *Bmpr1a* cKO females. Although ovaries from control and *Bmpr1a* cKO females contained follicles in all stages of development, most ovaries examined from 3-month-old *Bmpr1a* cKO mice contained a large number of growing follicles but fewer large antral follicles or corpora lutea compared with control ovaries (Fig. 3, A and B). In contrast, aside from the defects in cumulus expansion in *Bmpr1b*$^{-/-}$ mice, previous analysis of the ovaries from young adult females (5-wk-old) revealed no obvious abnormalities in follicular development or the number of corpora lutea (14). Our findings in ovaries from 3-month-old single BMPR1B mutant mice were similar; however, the ovaries from 3-month-old *Bmpr1b*$^{-/-}$ females were consistently smaller, and we frequently observed multi-oocyte follicles (MOFs) containing two oocytes within a single follicle boundary (Fig. 3, C and E). In addition, consistent with the findings in *Bmpr1b*$^{-/-}$ females (14), when we superovulated juvenile *Bmpr1a cKO Bmpr1b*$^{-/-}$ females and mated them to WT stud males of proven fertility, we recovered only unfertilized oocytes from the oviducts 34–36 h after hCG, whereas we recovered one- and two-cell embryos from our control and *Bmpr1a* cKO females animals (data not shown).

To evaluate redundant roles for BMPR1A and BMPR1B in the ovary, *Bmpr1a cKO Bmpr1b*$^{-/-}$ mice were generated. *Bmpr1a*$^{+/-}$ *Amhr2*$^{cre/+}$ mice were crossed to *Bmpr1b*$^{+/-}$ mice to obtain *Bmpr1a*$^{+/-}$ *Bmpr1b*$^{+/-}$ *Amhr2*$^{cre/+}$ mice, which were crossed to *Bmpr1a*$^{Flox/Flox}$ *Bmpr1b*$^{+/-}$ mice to obtain *Bmpr1a*$^{Flox/-}$ *Bmpr1b*$^{-/-}$ *Amhr2*$^{cre/+}$ double-mutant mice (designated *Bmpr1a Bmpr1b* dKO). Similar to the findings in *Bmpr1a* cKO females, ovaries from *Bmpr1a Bmpr1b* dKO females had an abundance of growing follicles (Fig. 3D). In addition, double-mutant ovaries contained MOFs, many zona pellucida remnants (ZPRs, markers of follicular atresia), and also abnormal follicle-like structures that were not observed in sin-

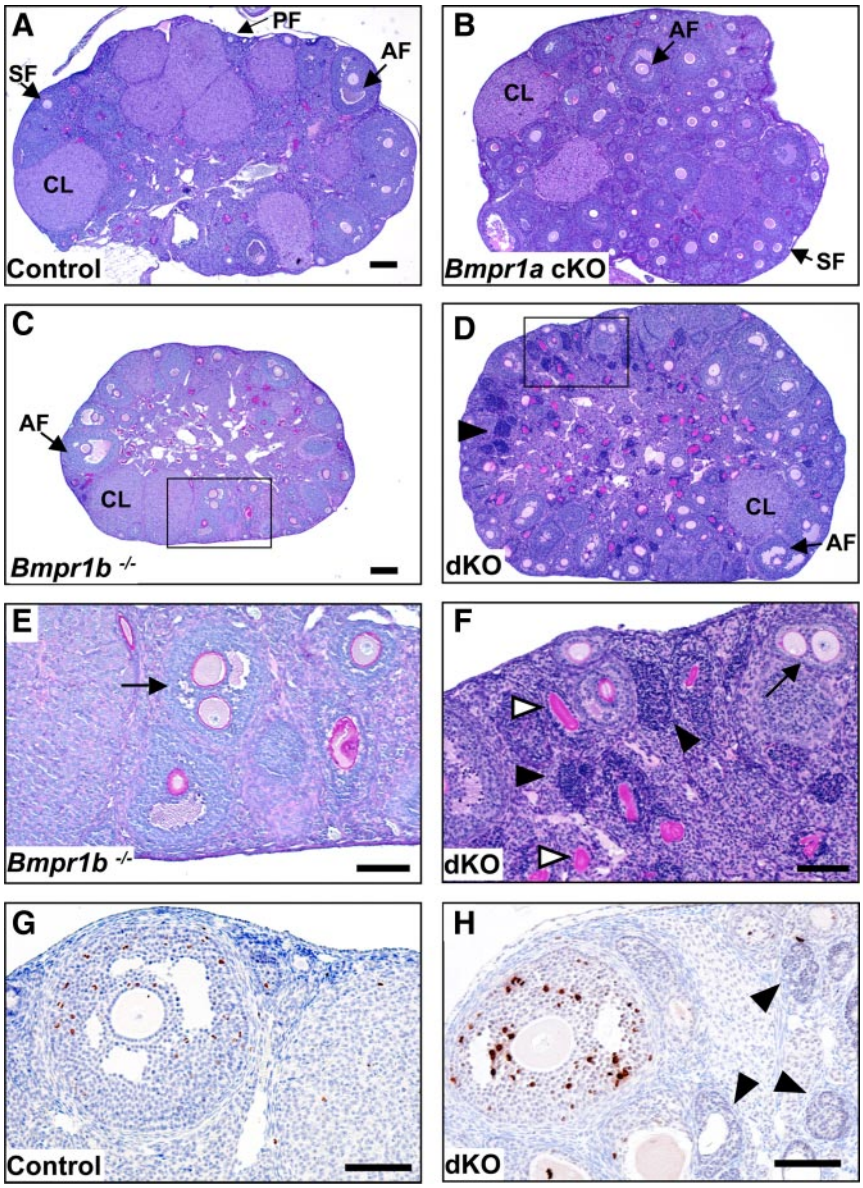

FIG. 3. Histological of analysis of control, *Bmpr1a* cKO, *Bmpr1b*$^{-/-}$, and *Bmpr1a Bmpr1b* dKO ovaries. Ovaries were collected from 3-month-old control and experimental mice and stained with periodic acid-Schiff and hematoxylin ($n \geq 5$ mice of each genotype). A, Normal histology of *Bmpr1a*$^{Flox/-}$ ovary containing follicles in all stages of development, including primary follicles (PF), secondary follicles (SF), and antral follicles (AF) as well as corpora lutea (CL); B, ovary from a *Bmpr1a* cKO female containing a large number of growing follicles and relatively few large antral follicles or corpora lutea; C and E, ovary from a *Bmpr1b*$^{-/-}$ female with follicles in all stages of development and containing a MOF (E, *arrow*); D and F, ovary from a *Bmpr1a Bmpr1b* dKO female with features of both *Bmpr1a* cKO and *Bmpr1b*$^{-/-}$ ovaries, including more growing follicles relative to antral follicles or corpora lutea, MOFs (*arrow*), ZPRs (*white arrowheads*), and abnormal follicle-like lesions (*black arrowheads*); G and H, phospho-histone H3 staining of control (G) and *Bmpr1a Bmpr1b* dKO ovaries (H) demonstrates proliferating granulosa cells in follicles of *Bmpr1a Bmpr1b* dKO ovaries but absence of proliferation in the follicle-like lesions (*arrowheads*). Magnification, ×25 (A–D; *scale bar*, 200 μm) and ×100 (E–H; *scale bar*, 100 μm).

gle *Bmpr1a* cKO or *Bmpr1b*$^{-/-}$ ovaries (Fig. 3F). Similar abnormal follicle-like lesions have been observed in ovaries of mice expressing dominant active Kirsten rat sarcoma viral oncogene homolog (30), and these structures had an increased expression of phosphatase and tensin homolog (25). The lesions in the *Bmpr1a Bmpr1b* dKO mutant mice, however, did not express elevated levels of phosphatase and tensin homolog (data not shown). Although immunostaining for the mitosis marker phospho-histone H3 suggested developing follicles in *Bmpr1a Bmpr1b* dKO ovaries had increased proliferation rates of granulosa cells compared with follicles in control ovaries, the cells in the follicle-like lesions were not proliferating (Fig. 3, G and H).

FSH and LH are pituitary gonadotropins that facilitate development of follicles beyond the preantral and ovulatory stages, respectively (7, 31, 32). To determine whether alterations in these hormones contribute to the follicular defects in *Bmpr1a* cKO and *Bmpr1a Bmpr1b* dKO ovaries, FSH and LH levels were measured in serum samples collected from randomly cycling 3-month-old control and mutant females. Levels of these hormones, however, were not different in single- or double-mutant females compared with control females (Table 1). In addition, although *in vitro* studies suggest BMPs inhibit progesterone production (33), our *in vivo* models demonstrate that serum progesterone is not altered in the absence of type I BMP receptors.

BMP signaling is markedly impaired in granulosa cells of *Bmpr1a Bmpr1b* dKO mutant mice

Although BMP15 preferentially signals through BMPR1B (17, 18), other BMPs in the ovary, such as BMP2 and BMP4, could potentially signal through either BMPR1A or BMPR1B (5, 34). We first determined the basal levels of known BMP target genes by QPCR assays in *Bmpr1a* cKO, *Bmpr1b*$^{-/-}$, and *Bmpr1a Bmpr1b* dKO granulosa cells. In granulosa cells from both single- and double-mutant mice, the basal levels of *Id3* were significantly decreased compared with granulosa cells from WT littermates, whereas *Id1* was significantly lower only in *Bmpr1a* cKO granulosa cells. The BMP antagonist *Grem1* was lower in *Bmpr1a Bmpr1b* dKO granulosa cells when compared

TABLE 1. Serum hormone profiles of control, *Bmpr1a* cKO, *Bmpr1b*$^{-/-}$, and *Bmpr1a Bmpr1b* dKO mice

Age group and genotype	FSH (ng/ml)	LH[a] (ng/ml)	P_4[a] (ng/ml)
3 months old			
Bmpr1a$^{Flox/-}$ (control)	7.05 ± 1.43[b] (11)	0.38 ± 0.08 (9)	10.59 ± 3.10 (10)
Bmpr1a cKO	6.70 ± 1.55[b] (11)	0.43 ± 0.08 (8)	9.81 ± 3.57 (7)
Bmpr1b$^{-/-}$	10.93 ± 1.49[b] (12)	0.16 ± 0.08 (9)	10.28 ± 1.94 (12)
Bmpr1a Bmpr1b dKO	6.03 ± 1.43[b] (9)	0.31 ± 0.07 (13)	5.59 ± 2.48 (12)
8–9 months old			
Bmpr1a$^{Flox/-}$ (control)	6.95 ± 1.86[b] (11)	0.26 ± 0.05 (10)	13.90 ± 5.29 (10)
Bmpr1a cKO	5.66 ± 1.59[b] (15)	0.31 ± 0.05 (13)	10.11 ± 2.71 (13)
Bmpr1b$^{-/-}$	4.90 ± 2.18[b] (8)	0.29 ± 0.06 (9)	7.78 ± 1.42 (9)
Bmpr1a Bmpr1b dKO	16.69 ± 2.33[c] (7)	0.43 ± 0.06 (7)	10.15 ± 3.27 (7)

Results are shown as the mean ± SEM for the indicated number of randomly cycling females (n). Data were analyzed by one-way ANOVA, followed by Tukey-Kramer honestly significant differences.

[a] $P > 0.05$.

[b] and [c] *Different letters* are significantly different at $P < 0.05$.

only with WT granulosa cells, whereas levels of the inhibitory SMAD, *Smad7*, were unchanged (Fig. 4A).

BMP4 and BMP2 are structurally similar to each other, and although binding to type I BMP receptors is likely cell type dependent, several studies suggest that these two BMPs bind to BMPR1A and/or BMPR1B with higher affinity than the other type I BMP receptor, ACVR1, which is preferentially bound by BMP6 and BMP7 (34–36). To examine the ability of BMPs to induce gene expression in the absence of BMPR1A, BMPR1B, or both of these receptors, granulosa cells from mice of all genotypes were treated with BMP4 or BMP2 for 5 h, and changes in the expression of *Id1*, *Id3*, *Smad7*, and *Grem1* were assessed (Fig. 4, B and C). After treatment with either BMP ligand, *Id1* induction was not significantly altered in *Bmpr1a* cKO or *Bmpr1b*$^{-/-}$ granulosa cells relative to WT granulosa cells. The expression of *Id3* in both *Bmpr1a* cKO and *Bmpr1b*$^{-/-}$ granulosa cells relative to WT granulosa cells was significantly lower after BMP4 treatment, whereas *Id3* was significantly increased in *Bmpr1b*$^{-/-}$ granulosa cells treated with BMP2. The fold induction of *Smad7* trended lower in BMP4-treated *Bmpr1b*$^{-/-}$ granulosa cells and was significantly lower in BMP2-treated *Bmpr1b*$^{-/-}$ granulosa cells. The induction of *Grem1* after BMP4 or BMP2 treatment was also blunted in granulosa cells from both *Bmpr1a* cKO and *Bmpr1b*$^{-/-}$ mice. In contrast to the variable changes in BMP target genes observed in *Bmpr1a* cKO or *Bmpr1b*$^{-/-}$ mice, there was a substantial reduction in the response to BMP4 and BMP2 in granulosa cells lacking both BMPR1A and BMPR1B, as shown by the significant differences in the induction of *Id1*, *Id3*, *Smad7*, and *Grem1* in *Bmpr1a Bmpr1b* dKO granulosa cells relative to WT granulosa cells (Fig. 4B). This suggests that in most cases, BMPR1B can partially compensate for BMPR1A, and vice versa, in activating pathways downstream of BMP4 and BMP2 in granulosa cells, but the absence of both receptors severely attenuates the response of granulosa cells to these BMPs.

Bmpr1a Bmpr1b dKO mice develop granulosa cell tumors

Based on the markedly reduced response of *Bmpr1a Bmpr1b* dKO granulosa cells to BMP4 and BMP2 and our previous observations that granulosa cell tumors develop in *Smad1 Smad5* cKO mice with 100% penetrance (10), we wanted to determine whether a BMP→BMPR1A/BMPR1B→SMAD1/5 pathway prevents tumorigenesis *in vivo*. Although tumors were evident in 100% of *Smad1 Smad5* cKO ovaries by 3 months (10), gross or histological evidence of tumors was not observed in *Bmpr1a Bmpr1b* dKO ovaries at this age, despite the presence of abnormal follicle-likes structures (Fig. 3D), which are not seen in *Smad1 Smad5* cKO ovaries (10). Ovaries from 8- to 9-month-old *Bmpr1a* cKO and *Bmpr1b*$^{-/-}$ single-mutant females generally exhibited signs of increased follicular atresia, as evident by abundant ZPRs, and by 8–9 months of age the majority of *Bmpr1b*$^{-/-}$ females had developed large epithelial-lined inclusion cysts (Fig. 5, A–D). Epithelial inclusion cysts arise from invaginations of the ovarian surface epithelium after ovulation and are believed to be precursors of epithelial ovarian cancers; however, no tumors were found in *Bmpr1b*$^{-/-}$ ovaries through 16 months of age (n = 6). Likewise, ovaries from 16-month-old *Bmpr1a* cKO females did not exhibit signs of malignancy (n =7). In contrast, by 8 months of age, about half of the *Bmpr1a Bmpr1b* dKO females developed ovarian tumors (Fig. 5E), and by 16 months of age, the majority of *Bmpr1a Bmpr1b* dKO females had developed large, often bilateral tumors (Fig. 5F).

Histological and immunohistochemical analyses of tumors from *Bmpr1a Bmpr1b* dKO females confirmed that

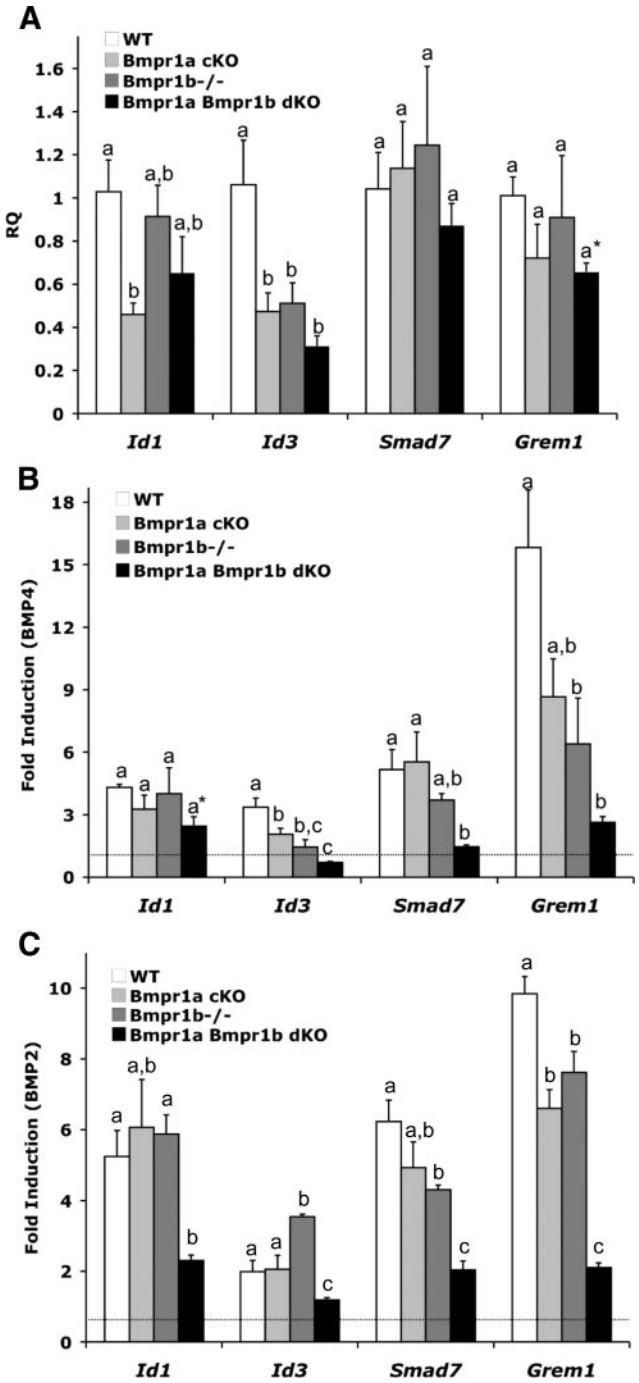

FIG. 4. Relative expression of BMP target genes in WT, *Bmpr1a* cKO, *Bmpr1b*$^{-/-}$, and *Bmpr1a Bmpr1b* dKO granulosa cells. Immature female mice (n = 4 for each genotype and at least three independent experiments) were primed with PMSG and granulosa cells were collected and cultured in the absence or presence of BMP4 (30 ng/ml) for 5 h. A, QPCR analysis of BMP target gene expression in untreated granulosa cells (RQ, relative quantity of transcript); B, QPCR analysis of gene expression changes after 5 h BMP4 treatment; C, QPCR analysis of gene expression changes after 5 h BMP2 treatment. Values are means ± SEM, relative to values for the WT group. Data were analyzed using one-way ANOVA and Tukey's honestly significant differences test. *Bars with a different letter* (a–c) are significantly different at $P < 0.05$. *Asterisks* denote statistical significance by two-tailed Student's *t* test relative to WT granulosa cells: *, $P \leq 0.01$.

these were granulosa cell tumors that were positive for inhibin-α (Fig. 6). The histological patterns of tumors ranged from poorly differentiated, with small, cuboidal granulosa cells arranged in sheets that were often punctuated by small follicle-like structures (Fig. 6A), to more differentiated, with plump granulosa cells containing a large amount of cytoplasm characteristic of luteinization (Fig. 6, C–E). In *Bmpr1a Bmpr1b* dKO tumors that also had large cysts, there were distinct boundaries of cytokeratin-8-positive epithelial cells lining the cysts and inhibin-α-positive tumor cells bordering these areas (Fig. 6, E and F), suggesting that the tumors were of granulosa cell origin, rather than epithelial origin. Finally, we also observed visible intraperitoneal metastases that were also positive for inhibin-α (Fig. 6, G and H); however, the incidence of metastases in *Bmpr1a Bmpr1b* dKO females was rare, in contrast to the frequent metastases observed in *Smad1 Smad5* cKO females (10).

Gene expression changes in *Bmpr1a Bmpr1b* dKO ovaries and tumors

To determine gene expression changes in pretumorigenic ovaries that might contribute to the development of tumors in older *Bmpr1a Bmpr1b* dKO females, candidate genes were evaluated in 3-month-old single- and double-mutant ovaries compared with WT littermates. Based on the increased proliferation observed in *Bmpr1a Bmpr1b* dKO ovaries (Fig. 2H), we first examined regulators of the cell cycle and observed a dose-dependent increase in cyclin D2 (*Ccnd2*) and cyclin E2 (*Ccne2*) mRNAs, with the largest relative increase occurring in *Bmpr1a Bmpr1b* dKO ovaries (Fig. 7, A and B). Levels of the protooncogene *Myc*, which also promotes cell cycle progression, were significantly increased in *Bmpr1a Bmpr1b* dKO ovaries (Fig. 7C). Cyclin D2 is induced by FSH signaling pathways (37), and despite no difference in serum FSH at 3 months of age in *Bmpr1a Bmpr1b* dKO females compared with control females (Table 1), *Fshr* was significantly elevated in *Bmpr1a Bmpr1b* dKO ovaries (Fig. 7D). In addition, by 8–9 months of age, serum FSH was also elevated in *Bmpr1a Bmpr1b* dKO females compared with both control and individual *Bmpr1a* cKO and *Bmpr1b*$^{-/-}$ females.

The deletion of BMPR1A and BMPR1B potentially results in a disproportionate activation of TGFβ/activin R-SMAD signaling pathways, and one regulator of *Fshr* expression in rat granulosa cells is TGFβ (38, 39). Although levels of *Tgfb1* were unchanged in 3-month-old *Bmpr1a Bmpr1b* dKO ovaries, *Tgfb2* trended higher ($P = 0.06$ *vs.* WT ovaries, data not shown), and there was evidence of an increased activation of TGFβ R-SMAD pathways, as determined by the mRNA levels of TGFβ-

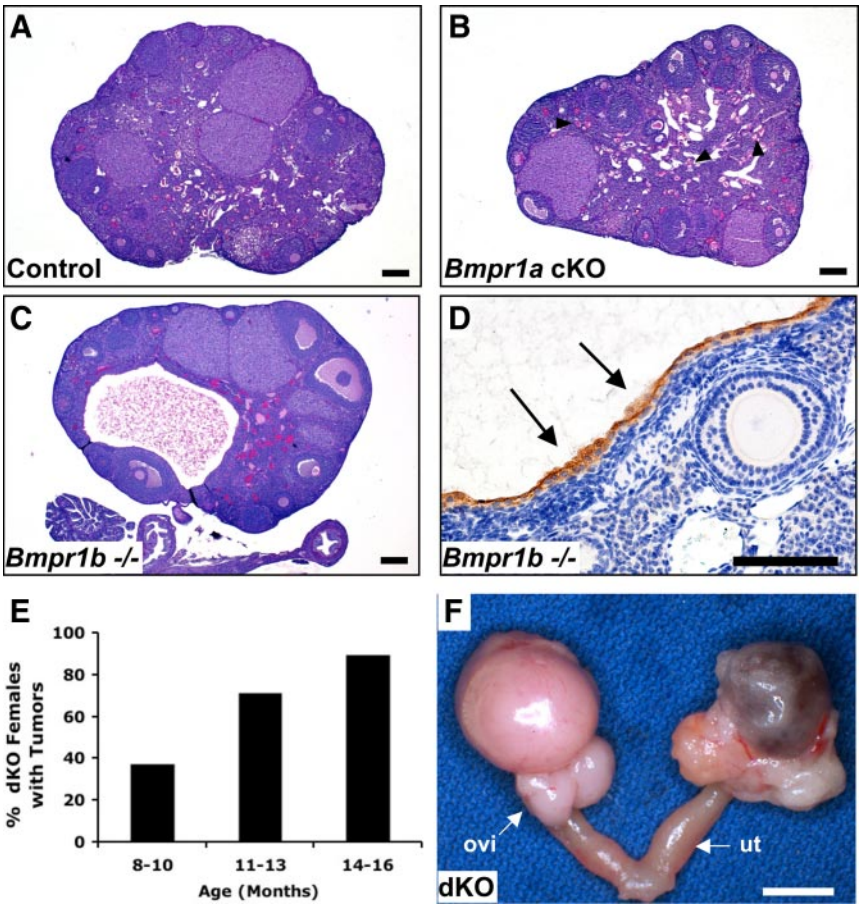

FIG. 5. Ovarian tumor development in *Bmpr1a Bmpr1b* dKO mice but not *Bmpr1a* cKO or *Bmpr1b*$^{-/-}$ mice. A, Ovary from a 9-month-old control female. B, Ovary from a 9-month-old *Bmpr1a* cKO female showing an abundance of ZPRs (*arrowheads*). C, Ovary from an 8-month-old *Bmpr1b*$^{-/-}$ female showing the formation of a large epithelial inclusion cyst. D, High-power magnification of a cyst from an 8-month-old *Bmpr1b*$^{-/-}$ female that is positive for cytokeratin 8 (*arrows*). E, Tumor incidence increases with age in *Bmpr1a Bmpr1b* dKO females. F, Bilateral tumor development in a 16-month-old *Bmpr1a Bmpr1b* dKO female. The tumor extends to the oviduct (ovi) but does not involve the uterus (ut). Magnification, ×25 (A–C) and ×200 (D). *Scale bars*, 200 μm (A–C), 100 μm (D), and 5 mm (F).

induced (*Tgfbi*), a TGFβ target gene (Fig. 7E). In *Bmpr1a Bmpr1b* dKO tumors, *Tgfb1* and *Tgfb2*, as well as *Tgfbi*, were significantly increased relative to WT granulosa cells (Table 2).

In addition to FSH regulation of cyclin D2, both cyclin D2 and cyclin E are induced by hedgehog signaling (40), and by microarray analysis, the hedgehog-regulated transcription factor *Gli1* was highly up-regulated in *Smad1 Smad5* cKO tumors compared with WT granulosa cells (10). Under normal conditions, the levels and activity of GLI transcription factors are positively regulated by hedgehog ligand binding to patched (PTCH) receptors, which leads to the activation of smoothened (SMO) receptors to influence GLI localization and expression. To determine whether alterations in hedgehog signaling may occur before tumor formation, the expression of several components of this pathway were examined in 3-month-old ovaries. Indian hedgehog (*Ihh*) and *Smo* as well as *Gli1* and *Gli2* were significantly increased in 3-month-old *Bmpr1a Bmpr1b* dKO ovaries (Fig. 8, A–D). Because *Gli1* and *Gli2* are also up-regulated by TGFβ in some cell types (41, 42), we evaluated whether TGFβ has a similar effect on granulosa cells. Wild-type granulosa cells were treated for 5 h in the presence or absence of TGFβ1, and both *Gli1* and *Gli2* were significantly up-regulated in the TGFβ1-treated compared with the untreated granulosa cells (Fig. 8, E and F). Although *Ihh* was not increased in granulosa cell tumors (data not shown), *Gli1* and *Gli2* remained elevated in granulosa cell tumors (Fig. 8G). A functional readout of GLI transcription factor activity is the up-regulation of PTCH receptors in a negative feedback loop (Fig. 8H). We found that *Ptch1* was also elevated in granulosa cell tumors relative to WT granulosa cells (Fig. 8G).

Finally, TGFβ signaling pathway genes and downstream targets of TGFβ that were altered in *Smad1 Smad5* cKO tumors (10) were evaluated in *Bmpr1a Bmpr1b* dKO tumors. With the exception of *Id1*, which was not significantly changed in *Bmpr1a Bmpr1b* dKO tumors, mRNAs for cartilage oligomeric protein (*Comp*) and *Grem1* were significantly decreased, whereas *Bmp7* was increased in *Bmpr1a Bmpr1b* dKO tumors, as was observed in *Smad1 Smad5* cKO tumors. Similarly, mRNAs for high-mobility group AT-hook 2 (*Hmga2*) and matrix metalloproteinase-2 (*Mmp2*), genes also activated by TGFβ pathways, were significantly up-regulated in *Bmpr1a Bmpr1b* dKO tumors. These gene changes are summarized in Table 2. Taken together, the molecular changes in *Bmpr1a Bmpr1b* dKO tumors support an early role for unopposed TGFβ signaling and dysregulation of hedgehog signaling in promoting granulosa cell tumor development when BMP signaling is compromised.

Although, in general, the *Bmpr1a Bmpr1b* dKO granulosa cell tumors and *Smad1 Smad5* cKO granulosa cell tumors molecularly phenocopied each other (Table 2), the *Smad1 Smad5* cKO phenotype was more severe in terms of tumor onset, penetrance, and development of metastases. These differences were not due to less efficient

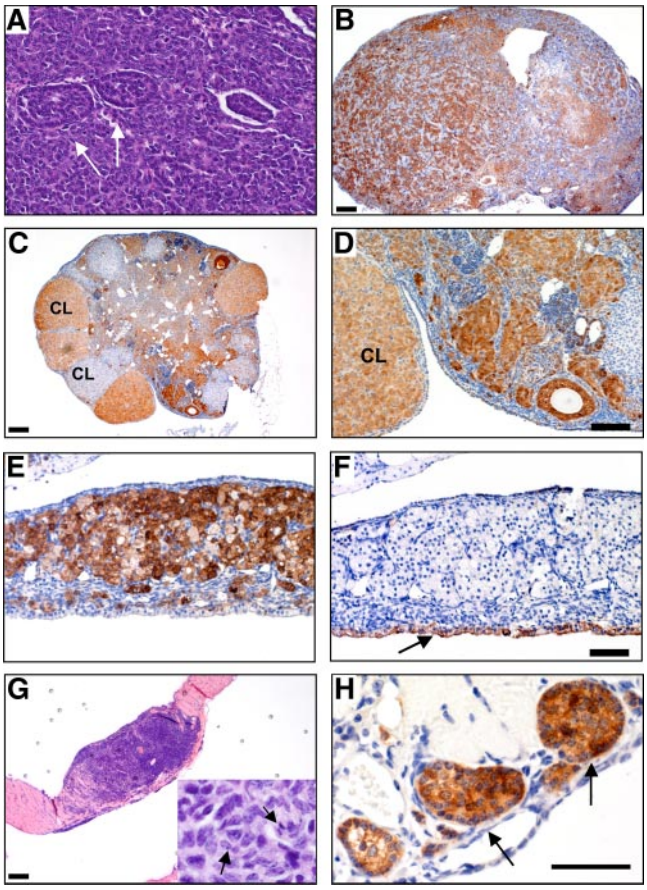

FIG. 6. *Bmpr1a Bmpr1b* dKO mice develop granulosa cell tumors A, High-power magnification of a granulosa cell tumor showing sheets of granulosa cells and follicle-like structures (*arrows*); B, ovary from a 12-month-old female showing replacement of the ovary with anastomosing cords of granulosa cells that are inhibin-α positive; C and D, inhibin-α immunoreactivity in an 8-month-old ovary demonstrating extensive tumor involvement of the ovarian stroma and positive staining in some corpora lutea (CL); E and F, high-power magnification of a serially sectioned cystic ovarian tumor from *Bmpr1a Bmpr1b* dKO female shows the tumor tissue is positive for inhibin-α (E), whereas the lining of the cyst is positive for cytokeratin 8 (*arrow*) (F); G, metastasis to the diaphragm in a 16-month-old female, with mitotic cells shown in the *inset* (*arrows*); H, diaphragm metastasis that is positive for inhibin-α (*arrows*). *Scale bars*, 200 μm (B, C, and G), 100 μm (D and F), and 50 μm (H).

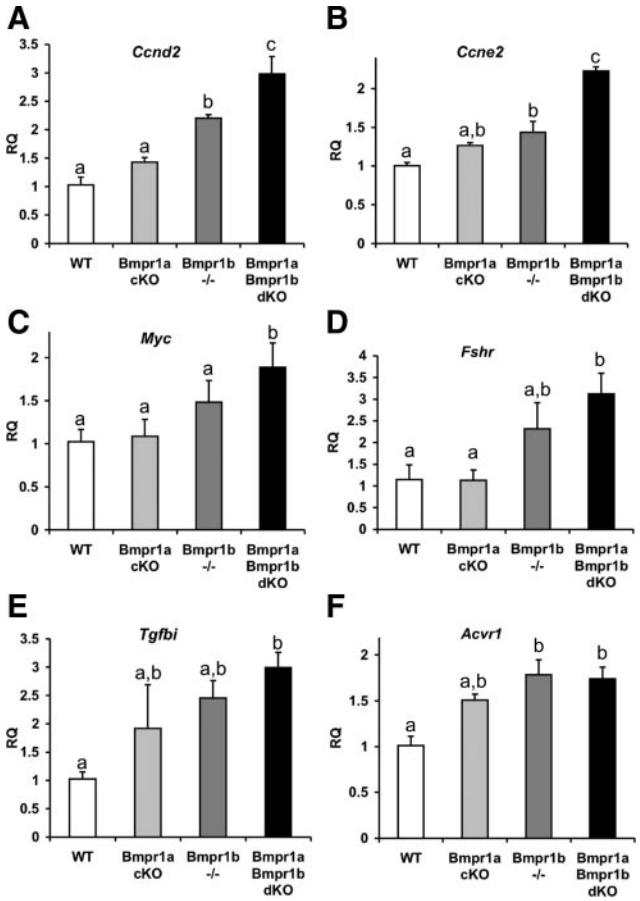

FIG. 7. Gene expression changes in *Bmpr1a* and *Bmpr1b* single- and double-mutant ovaries. A–E, QPCR analysis of candidate genes changes in 3-month-old ovaries from *Bmpr1a* cKO, *Bmpr1b*$^{-/-}$, and *Bmpr1a Bmpr1b* dKO compared with WT ovaries; F, QPCR analysis of *Acvr1* expression in granulosa cells from immature mice of the same genotypes. Data were analyzed using one-way ANOVA and Tukey's honestly significant differences test. *Bars with a different letter* (a–c) are significantly different at $P < 0.05$. RQ, Relative quantity of transcript.

recombination of the *Bmpr1a* floxed allele in the *Bmpr1b*$^{-/-}$ background. Specifically, the relative quantity of *Bmpr1a* in the *Bmpr1a Bmpr1b* dKO granulosa cells compared with *Bmpr1a*$^{Flox/+}$ granulosa cells was 0.18 ± 0.02 *vs.* 1.00 ± 0.04 (n = 5), which was not different from the relative quantity of *Bmpr1a* in granulosa cells from *Bmpr1a* cKO females (0.15 ± 0.02, Fig. 1A). To determine whether a compensatory increase in the remaining type I BMP receptor, ACVR1, in granulosa cells of the *Bmpr1a Bmpr1b* dKO mice could account for some of these discrepancies, we evaluated the expression of *Acvr1* by QPCR analysis. The levels of *Acvr1* showed a nearly 2-fold increase in *Bmpr1a Bmpr1b* dKO granulosa cells compared with control granulosa cells (Fig. 7F).

Discussion

We have previously shown that the combinatorial loss of SMAD1/5 in ovarian granulosa cells causes subfertility and leads to the development of metastatic granulosa cell tumors with features similar to the juvenile form of granulosa cell tumors in humans (10, 11). These findings suggest that at least one function of BMP signaling in granulosa cells is activation of tumor suppressor pathways and/or suppression of oncogenic pathways. Because of the early development of tumors in *Smad1 Smad5* cKO mice, and the fact that SMAD1/5 represent a convergence of all canonical BMP signaling pathways, the impact of one or more BMP family members and receptors on female fertility and in preventing tumorigenesis was unknown. The expression of various BMPs in multiple cell types and the embryonic or perinatal lethality of BMP2, BMP4, and BMP7 homozygous null mutant mice made addressing this question at the level of BMP ligands dif-

TABLE 2. Comparison of gene expression changes in *Smad1 Smad5* cKO and *Bmpr1a Bmpr1b* dKO tumors relative to WT granulosa cells

Gene	Change in *Smad1 Smad5* cKO tumor (10)	Fold change *Bmpr1a Bmpr1b* dKO tumor (QPCR)
Comp	↓↓	−430 ± 111[b]
Grem1	↓↓	−80.5 ± 21.5[b]
Id1	↓	No change
Tgfb1	Not shown	6.8 ± 1.4[b]
Tgfb2	Not shown	14.3 ± 5.2[a]
Tgfbi	↑↑	28.2 ± 4.9[b]
Bmp7	↑↑	21.9 ± 8.6[a]
Hmga2	↑↑	12.5 ± 3.2[a]
Mmp2	↑	282 ± 91[a]
Gli1	↑↑	5.1 ± 0.9[b]
Gli2	Not shown	8.0 ± 2.1[a]
Ptch1	Not shown	2.8 ± 0.5[a]

Arrows denote relative change previously reported (10). Results are shown as the mean ± SEM (n ≥ 5 independent granulosa cell or tumor samples).

[a] $P < 0.05$ (Student's *t* test).

[b] $P < 0.01$ (Student's *t* test).

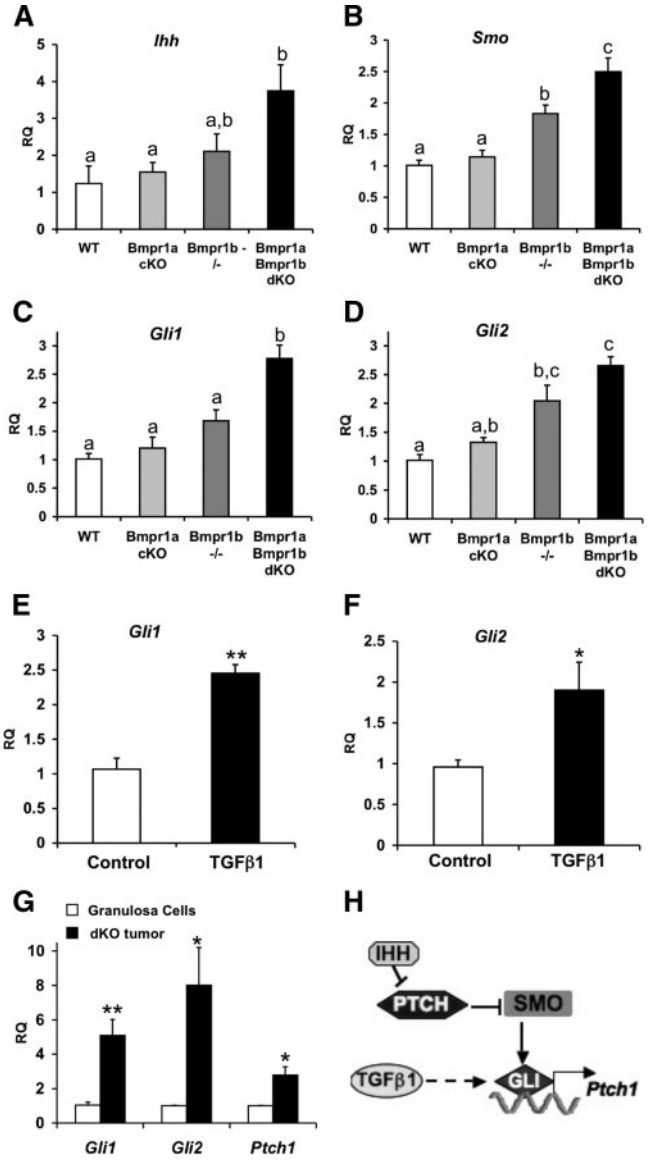

FIG. 8. Hedgehog signaling components are altered in pretumorigenic *Bmpr1a Bmpr1b* dKO ovaries and remain elevated in tumors. A–D, QPCR analysis of components of the hedgehog signaling pathway in 3-month-old ovaries from *Bmpr1a* cKO, *Bmpr1b*$^{-/-}$, and *Bmpr1a Bmpr1b* dKO compared with WT ovaries; E and F, QPCR analysis of *Gli1* and *Gli2* expression in granulosa cells from immature WT mice that were cultured for 5 h in the absence (control) or presence of TGFβ1 (30 ng/ml); G, QPCR analysis of GLI transcription factors and GLI target gene *Ptch1* in *Bmpr1a Bmpr1b* dKO granulosa cell tumors compared with WT granulosa cells; H, summary of hedgehog signaling pathway. Hedgehog ligands bind to PTCH receptors leading to depression of SMO and activation of GLI transcription factors, which regulate a number of target genes, one of which is *Ptch1*. TGFβ1 up-regulates the expression of GLI transcription factors. Data in A–D were analyzed using one-way ANOVA and Tukey's honestly significant differences test, and *bars with a different letter* (a–c) are significantly different at $P < 0.05$. *Asterisks* (E–G) denote statistical significance by two-tailed Student's *t* test: *, $P < 0.05$; **, $P < 0.01$. RQ, Relative quantity of transcript.

ficult. An alternative approach for beginning to decipher BMP functions in ovarian biology *in vivo* is to delete BMP receptors. The sterility and cumulus cell defects in BMPR1B-deficient female mice (14) suggested BMPR1A might have nonredundant functions in follicular development and fertility. To evaluate potentially unique functions for BMPR1A in granulosa cells, we first generated *Bmpr1a* cKO female mice, which were subfertile with significantly smaller litters and fewer litters per month. Despite the presence of a large number of growing follicles in ovaries from 12-wk-old *Bmpr1a* cKO mice, the spontaneous ovulation rate, as measured by the recovery of blastocysts from the reproductive tracts of *Bmpr1a* cKO and control females, was reduced. Cumulus expansion, however, was not impaired and the developmental competence of ovulated oocytes was intact, because there was not a difference in the number of blastocysts in relation to unfertilized oocytes or degenerating embryos in *Bmpr1a* cKO *vs.* control females (data not shown). Moreover, the robust response in the artificial induction of decidualization in *Bmpr1a* cKO females suggests that uterine defects did not contribute to the subfertility phenotype. Thus, in contrast to *Bmpr1b*$^{-/-}$ females, which do not differ from controls in the number of oocytes spontaneously ovulated but have defects in cumulus expansion (14), *Bmpr1a* cKO females have a reduction in spontaneous ovulation but normal cumulus expansion.

In addition to BMPs, granulosa cells in developing follicles are exposed to anti-Müllerian hormone (AMH), TGFβs, activins, inhibins, and GDF9. In AMH-deficient mice, there is an increased rate of recruitment of primordial follicles into the growing pool, but the mice do not exhibit fertility defects until a very advanced age (44). Although BMPR1A is one of the type I receptors for AMH, BMPR1A and the other type I receptor, ACVR1,

generally function redundantly during AMH-mediated regression of the Müllerian duct in male mice (45). In addition, as mentioned in *Results*, *Bmpr1a*$^{+/-}$ *Amhr2*$^{cre/+}$ females that were used to generate *Bmpr1a* cKO mice had normal fertility. Thus, haploinsufficiency for both the type II AMH receptor and one of two type I AMH receptors does not cause fertility defects. Moreover, *Amhr2*-Cre is not highly expressed until the secondary stage of folliculogenesis, suggesting the abundance of secondary follicles observed when *Bmpr1a* is deleted in granulosa cells might be partially, but not entirely, due to disruption of AMH signaling. Instead, we hypothesize that ablation of BMPR1A in granulosa cells might shift the balance toward relatively more TGFβ/activin signaling and less BMP signaling, contributing to the altered follicular development in *Bmpr1a* cKO mice. For example, activin A has been shown to cause preantral follicles to remain dormant *in vitro* (46), suggesting that it is preventing the follicles from further developing and differentiating. However, the effects are different in preantral follicles from adult *vs.* immature mice where follicles from the former are inhibited by activin A and those from the latter increase in size when exposed to activin A (47). We have previously shown that loss of intraovarian activins in adult mice causes an increase in antral follicles and corpora lutea (48), although the increase in corpora lutea is most likely due to defective structural regression. Thus, *in vitro* studies of adult preantral follicles and our previous *in vivo* analysis of activin-deficient mice suggest that one of the consequences of an increase in activin signaling relative to BMP signaling in *Bmpr1a* cKO mice could be a partial block in preantral to antral follicular development, contributing to fewer ovulated oocytes during each estrous cycle.

In addition to the defects in cumulus expansion previously reported in *Bmpr1b*$^{-/-}$ female mice (14), our histological analysis of BMPR1B-deficient ovaries from young adult females demonstrated a frequent occurrence of MOFs (Fig. 3). MOFs have also been observed in several transgenic mouse lines with disrupted TGFβ superfamily signaling in the ovary, including BMP15-null mice (49), activin-βA cKO mice (48), inhibin-α-overexpressing mice (50), and germ cell nuclear factor cKO mice (51). However, it is likely that MOFs arise through multiple mechanisms, because these mouse lines do not uniformly disrupt only SMAD1/5 or only SMAD2/3 signaling. Moreover, although MOF formation is believed to occur secondarily to incomplete breakdown of germ cell clusters during follicle assembly, which occurs postnatally in mice and has been linked to prenatal or neonatal estrogen exposure (reviewed in Ref. 7), MOFs have also been attributed to follicle joining after germ cell cluster breakdown when oocyte glycoprotein assembly is disrupted (52).

The principle finding of this study was that BMPR1A and BMPR1B have redundant functions in preventing the development of granulosa cell tumors. Although no *Bmpr1a* cKO or *Bmpr1b*$^{-/-}$ single-mutant female mice developed malignancies through 16 months of age, the majority (~90%) of *Bmpr1a Bmpr1b* dKO mice developed tumors by this age. A redundant role for both receptors in transmitting some BMP signals is further supported by the observation that the response to BMP4 and BMP2 is largely intact when only BMPR1A or BMPR1B is deleted but is markedly attenuated or eliminated when both BMPR1A and BMPR1B are deleted in granulosa cells (Fig. 4). Although the development of granulosa cell tumors in *Bmpr1a Bmpr1b* dKO mice is similar to the *Smad1 Smad5* cKO model (10), there are some differences in ablation of BMP R-SMADs *vs.* BMP receptors. *Smad1 Smad5* cKO female mice develop granulosa cell tumors with 100% penetrance and at a younger age than *Bmpr1a Bmpr1b* dKO mice. The incidence of intraperitoneal tumor metastasis is also relatively low in *Bmpr1a Bmpr1b* dKO mice. A number of factors may contribute to these findings. Conditional ablation of BMPR1A reduces the *Bmpr1a* transcript levels to about 15%; the very low levels of BMPR1A remaining may cause some activation of SMAD1/5 pathways and be sufficient to delay tumorigenesis. In addition to BMPR1A and BMPR1B expression in granulosa cells, by semiquantitative RT-PCR, we detected the other type I BMP receptor, *Acvr1*, in WT granulosa cells (data not shown), and by QPCR analysis, *Acvr1* was significantly increased in *Bmpr1a Bmpr1b* dKO granulosa cells as compared to WT. Thus, ACVR1 may also maintain a certain level of BR-SMAD activity to delay tumorigenesis and, in addition, perhaps oppose metastasis.

BMPR1A and BMPR1B are similar in structure and are preferentially bound by BMP2 and BMP4 (34). In addition, oocyte-secreted BMP15 preferentially binds to BMPR1B (18). BMP6 and BMP7, on the other hand, bind to ACVR1 with higher affinity than BMPR1A or BMPR1B (53, 54); however, these binding profiles may differ depending on the cellular context and the type II receptors present on a cell (36). Notably, all of these BMPs are expressed in rodent ovarian follicles, and there is particularly high expression of BMP2 in granulosa cells of atretic follicles (12, 13). Our *in vitro* culture experiments demonstrate a markedly blunted response to recombinant BMP2 in *Bmpr1a Bmpr1b* dKO granulosa cells compared with WT granulosa cells (Fig. 3C). Thus, it is possible that the abnormal follicle-like lesions observed in *Bmpr1a Bmpr1b* dKO mice, which morphologically

appear to be follicular remnants because some contain ZPRs (Fig. 3F), result from an impaired response to BMP2 during follicular atresia, a process that normally results in the clearing of all somatic cells, leaving behind a ZPR. It is currently unclear whether these follicle-like lesions contribute to tumorigenesis, because they do not appear to have proliferating cells (Fig. 3H); however, by cleaved caspase 3 staining, the cells also do not appear to be apoptotic (data not shown).

In addition to canonical BMP signaling through BR-SMADs, there is considerable evidence that the TGFβ receptors activate non-SMAD pathways (55). Although we believe our current findings, in conjunction with our previous findings (10), strongly implicate that BMP signaling through the BR-SMAD axis functions as a tumor suppressor pathway in granulosa cells, additional studies suggest BMP receptors can also activate MAPK and AKT mitogenic pathways independent of BR-SMAD activation (55). In the absence of concurrent activation of BR-SMADs in promoting differentiation, BMP mitogenic signals, in cooperation with unopposed AR-SMAD signaling, might more rapidly tip the balance in favor of proliferation in *Smad1 Smad5* cKO mice. Thus, we postulate that ablation of BMPR1A and BMPR1B receptors in the present study not only severely reduces the propagation of differentiation signals via BR-SMADs but could also decrease mitogenic signals through noncanonical pathways downstream of the type I receptors, thus contributing to the differences in tumor onset and metastasis *vs.* *Smad1 Smad5* cKO mice.

A number of mouse models have now been generated that support a role for dysregulated TGFβ/activin signaling through AR-SMADs in the development of granulosa cell tumors (7). Mice lacking inhibin-α (*Inha*$^{-/-}$) are completely deficient in inhibins, and both males and females develop sex cord-stromal tumors at an early age (56), eventually dying secondarily to a cachexia wasting syndrome (57). Immunostaining of ovarian tumors in *Inha*$^{-/-}$ females shows evidence of increased SMAD2/3 activation (11), and deletion of SMAD3 in *Inha*$^{-/-}$ females decreases ovarian tumor progression and increases survival (58). In addition, administering a chimeric type II ACVR antagonist (ACVR2A-mFc) prevents the cachexia syndrome and delays tumor progression (58, 59). These previous studies, the findings in *Smad1 Smad5* cKO mice, and our present observations with *Bmpr1a Bmpr1b* dKO mice strongly support the notion that unopposed TGFβ/activin signaling promotes granulosa cell tumorigenesis. Moreover, our findings further suggest that an imbalance of TGFβ/activin signaling leads to an increase in mediators of hedgehog signaling, including *Gli1* and *Gli2*, that may contribute to tumor formation and progression. Elevated components of hedgehog signaling have also been detected in a mouse model of skin tumorigenesis mediated by overexpression of the BMP antagonist Noggin (60), which has a similar effect on BMP signaling as ablation of BMP receptors.

In canonical hedgehog signaling, activation of GLI transcription factors requires binding of hedgehog ligands to transmembrane PTCH receptors (PTCH1 and PTCH2), which normally repress the activity of the SMO receptor. Hedgehog binding inhibits PTCH activity, causing depression of SMO, ultimately regulating the levels and activity of GLI proteins. Aberrant activation of this pathway is associated with various cancers (61), including epithelial ovarian cancers (61, 62). Although PTCH1 in the ovary appears predominantly localized to the theca, with Indian hedgehog highly expressed in granulosa cells (63), PTCH1 and SMO have also been detected in granulosa cells (63, 64). In addition, TGFβ induces *Gli1* and *Gli2* expression in a number of cell types in a SMAD3-dependent fashion (41); we found that TGFβ also regulates *Gli1* and *Gli2* in granulosa cells. Moreover, recent work in a pancreatic cancer model suggests GLI1 target genes are regulated in a SMO-independent manner through noncanonical regulation by TGFβ and Kirsten rat sarcoma viral oncogene homolog (42). Because *Ihh* did not remain elevated in granulosa cell tumors *Bmpr1a Bmpr1b* dKO females compared with WT granulosa cells, yet there was an increase in *Tgfb1* and *Tgfb2* as well as several TGFβ target genes (Table 2), a similar noncanonical regulation of GLI activity and levels may also occur in our model of granulosa cell tumorigenesis.

In addition to identifying unique functions for BMPR1A in female fertility, our findings solidify the notion that a BMP→BMPR1A/BMPR1B→SMAD1/5 signaling axis acts as a tumor suppressor in mouse granulosa cells. In humans, *BMPR1A* mutations have been associated with juvenile polyposis and an increased risk of gastrointestinal cancer (65, 66), and *BMPR1B* is epigenetically silenced in some patient-derived, tumor-initiating glioblastoma cell lines (67). It is possible that function-disrupting mutations of *BMPR1A* and/or *BMPR1B* contribute to the development of granulosa cell tumors in humans. Our present data, and other recent findings (10, 60), demonstrate that one of the consequences of disrupted BMP signaling is an increase in components of hedgehog signaling, suggesting combinatorial therapeutic approaches to antagonize both TGFβ and hedgehog signaling in certain cancers may be beneficial.

Materials and Methods

Generation and genotyping of *Bmpr1a* cKO mice and *Bmpr1a* cKO; *Bmpr1b*$^{-/-}$ mice

All mouse lines in the present study were maintained on a C57BL/6J;129S5/SvEvBrd mixed hybrid background in accordance with the National Institutes of Health Guide for the Care and Use of Laboratory Animals. The *Bmpr1a*-null allele

(*Bmpr1a*$^{-}$) and the *Bmpr1a* conditional allele with the second coding exon (exon 4) flanked by *loxP* sites (*Bmpr1a*^{Flox}) have previously been described (19, 21). The *Bmpr1b*-null allele (*Bmpr1b*$^{-}$) has also been described (68). To generate *Bmpr1a*-deficient granulosa cells, *Bmpr1a*$^{+/-}$ mice were bred to *Amhr2*$^{cre/+}$ mice (20), and the resulting *Bmpr1a*$^{+/-}$;*Amhr2*$^{cre/+}$ offspring were then bred to *Bmpr1a*$^{Flox/Flox}$ mice to generate *Bmpr1a*$^{Flox/-}$ *Amhr2*$^{cre/+}$ experimental mice (designated throughout as *Bmpr1a* cKO). *Bmpr1a* cKO;*Bmpr1b*$^{-/-}$ animals were obtained by crossing *Bmpr1a*$^{Flox/Flox}$;*Bmpr1b*$^{+/-}$ mice with *Bmpr1a*$^{+/-}$;*Bmpr1b*$^{+/-}$;*Amhr2*$^{cre/+}$ mice. Tail genomic DNA was used for PCR genotyping of all alleles according to the manufacturer's protocol (New England Biolabs, Ipswich, MA). Primers used for the *Bmpr1a*-null allele were FX3 (5′-AGACTGCCTTGGGAAAAGCGC-3′) (19) and R1 (5′-CTGCCCCAAGGAACTTGATG-3′). The *Bmpr1b*-null and *Bmpr1b* WT alleles were detected using the following primers in a multiplex reaction: *Bmpr1b*-WT-fwd (5′-atgtgggcaccaagaaggaggat-3′) (68), *Neo* (5′-tagttgccagccatctgttgtt-3′), and *Bmpr1b*-rev (5′-gagtggttacaacaagatcagca). Primers used for *Amhr2*$^{cre/+}$ were *Amhr2*-Cre F1 (5′-CGCATTGTCTGAGTAGGTGT-3′) and *Amhr2*-Cre R2 (5′-AGAGAGGCTGCGTTGAGTGT-3′). Recombination of the *Bmpr1a* floxed allele was confirmed by QPCR analysis of *Bmpr1a* transcript levels in granulosa cell cDNA using a predesigned TaqMan Assay-On-Demand (Applied Biosystems, Foster City, CA) with primers spanning the floxed allele (Mm00477650_m1).

Fertility analysis and estrous cycle monitoring

To assess reproductive performance of *Bmpr1a* cKO female mice, six individually housed 6-wk-old *Bmpr1a*$^{Flox/-}$ control and *Bmpr1a* cKO littermates were bred to WT C57BL/6J; 129S5/SvEvBrd hybrid males with known fertility. The number of litters and pups born per litter were recorded over the course of 6 months.

To evaluate estrous cyclicity in a separate group of 6- to 8-wk-old control and *Bmpr1a* cKO mice, vaginal smears were collected each day between 1200 and 1300 h over a 1-month period. Smears were diluted in PBS, examined under a light microscope, and classified into one of four phases of the estrous cycle (proestrus, estrus, metestrus, or diestrus) as described elsewhere (69). Estrous cycles were monitored over an additional 1-month period in the same group of mice beginning at approximately 7 months of age.

Ovulation assays

Superovulation of 21- to 25-d-old mice was performed as described elsewhere (69, 70). Briefly, mice were injected with 5 IU PMSG (Calbiochem, La Jolla, CA), followed 44–46 h later by 5 IU hCG (Novarel; Ferring Pharamaceuticals, Parsippany, NJ). COCs were recovered from the ampulla of the oviducts 16–18 h after hCG and evaluated for cumulus expansion before transfer to M2 medium containing 0.5 mg/ml hyaluronidase (Sigma Chemical Co., St. Louis, MO) for dissociation of cumulus cells to facilitate counting. Spontaneous ovulation was determined by housing 9- to 16-wk-old adult females with WT males of known fertility. Females with a copulatory plug were euthanized 3.5 d after coitus, uterine horns were flushed with M2, and blastocysts, unfertilized oocytes, or degenerating embryos were quantified.

Artificial induction of decidualization

The uterine decidual response was determined as described previously, with minor modifications (70). Briefly, after hormonal priming of ovariectomized mice, one uterine horn was traumatized by intraluminal scratching five times with a 26-gauge needle. The contralateral horn was not scratched and served as a control. Mice continued to receive sc injections of 1 mg progesterone (Sigma) and 6.7 ng 17β-estradiol (Sigma) for 5 d after the trauma, at which point they were anesthetized and killed by cervical dislocation.

Histology and immunohistochemistry

Ovaries from mice of various ages were either fixed overnight in 10% neutral buffered formalin and then transferred to 70% ethanol or snap frozen at −80 C. Tissue processing and embedding were performed by the Department of Pathology Core Services Laboratory (Baylor College of Medicine, Houston, TX). Five-micrometer sections were stained with either periodic acid-Schiff reagent and hematoxylin counterstain, or hematoxylin-eosin using standard techniques. Immunohistochemistry was performed using the Vectastain ABC kit (Vector Laboratories, Inc., Burlingame, CA) as described previously (6). Primary antibodies were diluted as follows: rabbit polyclonal phosphohistone H3 (Ser 10) (Cell Signaling Technology, Beverly, MA), 1:300; rabbit polyclonal inhibin-α (a gift of W. Vale, Salk Institute, La Jolla, CA), 1:500; rat monoclonal Troma-I (cytokeratin-8, obtained from the Developmental Studies Hybridoma Bank developed under the auspices of the National Institute of Child Health and Human Development and maintained by the University of Iowa Department of Biological Sciences, Iowa City, IA), 1:200. After overnight incubation with primary antibodies, samples were incubated with the appropriate biotinylated secondary antibody (Vector Laboratories) at 1:200 for 1 h, and immunoreactivity was visualized by diaminobenzidine tetrahydrochloride staining. Tissues were counterstained in hematoxylin.

Serum hormonal analysis

Randomly cycling 12-wk-old mice were anesthetized with isoflurane (Abbott Laboratories, Chicago, IL), and blood was collected by cardiac puncture. Serum was prepared using microtainer tubes (Becton and Dickinson, Franklin Lakes, NJ) and stored at −20 C until further use. FSH, LH, and progesterone measurements were performed by the University of Virginia Ligand Core Facility (Charlottesville, VA).

Granulosa cell cultures and ligand treatment

Collection and treatment of granulosa cells from immature WT and experimental animals were performed as previously described (10, 69). Mice were injected at 21–25 d of age with 5 IU PMSG, and granulosa cells were obtained by antral follicle puncture 44–46 h later. Cells from individual animals were resuspended in DMEM-F-12 (Invitrogen, Carlsbad, CA) supplemented with 0.5% heat-inactivated fetal bovine serum and 10 U/ml penicillin and streptomycin and equally divided into control and treated groups in 24-well plates. Cells were treated with BMP4 (30 ng/ml; R&D, Minneapolis, MN), BMP2 (100 ng/ml; R&D), or TGFβ1 (30 ng/ml; R&D) for 5 h and then harvested for RNA.

RNA analysis

RNA was extracted using a RNeasy Micro kit (QIAGEN, Valencia, CA) with on-column deoxyribonuclease digestion of genomic DNA, according to the manufacturer's instructions. cDNA was prepared from 250 ng total RNA in a 25-μl reaction using a Superscript III first-strand synthesis kit (Invitrogen). Granulosa cell samples were diluted 20-fold, and 5 μl was used in a 20 μl QPCR, which was performed on an ABI prism 7500 sequence detection system (Applied Biosystems) as described previously (8). The following predesigned TaqMan gene expression assays (Applied Biosystems) were used: *Id1*, Mm00775963_g1; *Id3*, Mm00492575_m1; *Smad7*, Mm00484742_m1; *Grem1*, Mm00488615_s1; *Ccnd2*, Mm00438071; *Ccne2*, Mm00438081_m1; *Myc*, Mm00487804_m1; *Fshr*, Mm00442819_m1; *Tgfb1*, Mm00441724_m1; *Tgbf2*, Mm01321739_m1; *Tgfbi*, Mm00493644_m1; *Acvr1*, Mm01331067_m1; *Ihh*, Mm01259021_m1; *Smo*, Mm01162710_m1; *Gli1*, Mm00494646_g1; *Gli2*, Mm01293117_m1; *Ptch1*, Mm00436014_m1; *Comp*, Mm00489496_m1; *Hmga2*, Mm00780304_sH; *Bmp7*, Mm00432102_m1; and *Mmp2*, Mm00439508_m1. The relative quantity of transcript was normalized to an endogenous control (*Gapdh*) calculated according to the $2^{-\Delta\Delta CT}$ method (43).

Statistical analysis

Data are presented as the mean ± SEM. JMP version 8.0 software (SAS Software, Cary, NC) was used for statistical analysis. Differences between groups were evaluated using the Student's *t* test for single comparisons or one-way ANOVA followed by Tukey's honestly significant differences test for multiple comparisons. $P < 0.05$ was considered statistically significant.

Acknowledgments

We thank Richard Behringer for the *Bmpr1a*$^{+/-}$, *Bmpr1a*^{Flox}, and *Amhr2-Cre* mice, Wylie Vale for the inhibin-α antibody, Xiaohui Li and Julio Agno for genotyping assistance, Lang Ma for tissue-sectioning assistance, and Ruihong Chen for periodic acid-Schiff staining. We also thank the University of Virginia Ligand Assay and Analysis Core (Specialized Cooperative Centers Program in Reproduction Research, Charlottesville, VA) for performing serum hormone assays and Michelle Myers for discussions and critical reading of the manuscript.

Address all correspondence and requests for reprints to: Martin M. Matzuk, M.D., Ph.D., The Stuart A. Wallace Chair and Professor, Department of Pathology, Baylor College of Medicine, One Baylor Plaza, Houston, Texas 77030. E-mail: mmatzuk@bcm.edu.

This work was supported by National Institutes of Health (NIH) Grants HD32067 (to M.M.M.), AR44528 (to K.M.L), T32GM07730 (to M.A.E.), and T32HD007165 (to M.A.E. and H.L.F.); a scholarship from Baylor Research Advocates for Student Scientists (to M.A.E. and H.L.F.); and a Burroughs Welcome Career Award in Biomedical Sciences, the Caroline Weiss Law Fund for Molecular Medicine, and the L. E. and Josephine S. Gordy Memorial Career Research Fund (to S.A.P). The University of Virginia Ligand Assay and Analysis Core (Specialized Cooperative Center Program in Reproduction and Infertility Research) is supported by (NIH) Grant U54 HD28934.

Disclosure Summary: The authors have nothing to disclose.

References

1. **Chang H, Brown CW, Matzuk MM** 2002 Genetic analysis of the mammalian TGF-β superfamily. Endocr Rev 23:787–823
2. **Pangas SA, Matzuk MM** 2008 The TGF-β family in the reproductive tract. In: Derynck R, Miyazono K, eds. The TGF-β family. Cold Spring Harbor, NY: Cold Spring Harbor Laboratory Press; 861–888
3. **Schmierer B, Hill CS** 2007 TGFβ-SMAD signal transduction: molecular specificity and functional flexibility. Nat Rev Mol Cell Biol 8:970–982
4. **Miyazono K, Kamiya Y, Morikawa M** 2010 Bone morphogenetic protein receptors and signal transduction. J Biochem 147:35–51
5. **Chen D, Zhao M, Mundy GR** 2004 Bone morphogenetic proteins. Growth Factors 22:233–241
6. **Nalam RL, Andreu-Vieyra C, Braun RE, Akiyama H, Matzuk MM** 2009 Retinoblastoma protein plays multiple essential roles in the terminal differentiation of Sertoli cells. Mol Endocrinol 23:1900–1913
7. **Edson MA, Nagaraja AK, Matzuk MM** 2009 The mammalian ovary from genesis to revelation. Endocr Rev 30:624–712
8. **Li Q, Pangas SA, Jorgez CJ, Graff JM, Weinstein M, Matzuk MM** 2008 Redundant roles of SMAD2 and SMAD3 in ovarian granulosa cells in vivo. Mol Cell Biol 28:7001–7011
9. **Pangas SA, Li X, Robertson EJ, Matzuk MM** 2006 Premature luteinization and cumulus cell defects in ovarian-specific Smad4 knockout mice. Mol Endocrinol 20:1406–1422
10. **Pangas SA, Li X, Umans L, Zwijsen A, Huylebroeck D, Gutierrez C, Wang D, Martin JF, Jamin SP, Behringer RR, Robertson EJ, Matzuk MM** 2008 Conditional deletion of Smad1 and Smad5 in somatic cells of male and female gonads leads to metastatic tumor development in mice. Mol Cell Biol 28:248–257
11. **Middlebrook BS, Eldin K, Li X, Shivasankaran S, Pangas SA** 2009 Smad1-Smad5 ovarian conditional knockout mice develop a disease profile similar to the juvenile form of human granulosa cell tumors. Endocrinology 150:5208–5217
12. **Erickson GF, Shimasaki S** 2003 The spatiotemporal expression pattern of the bone morphogenetic protein family in rat ovary cell types during the estrous cycle. Reprod Biol Endocrinol 1:9
13. **Shimasaki S, Moore RK, Otsuka F, Erickson GF** 2004 The bone morphogenetic protein system in mammalian reproduction. Endocr Rev 25:72–101
14. **Yi SE, LaPolt PS, Yoon BS, Chen JY, Lu JK, Lyons KM** 2001 The type I BMP receptor BmprIB is essential for female reproductive function. Proc Natl Acad Sci USA 98:7994–7999
15. **Yoon BS, Ovchinnikov DA, Yoshii I, Mishina Y, Behringer RR, Lyons KM** 2005 Bmpr1a and Bmpr1b have overlapping functions and are essential for chondrogenesis in vivo. Proc Natl Acad Sci USA 102:5062–5067
16. **Yoon BS, Pogue R, Ovchinnikov DA, Yoshii I, Mishina Y, Behringer RR, Lyons KM** 2006 BMPs regulate multiple aspects of growth-plate chondrogenesis through opposing actions on FGF pathways. Development 133:4667–4678
17. **Li Q, Rajanahally S, Edson MA, Matzuk MM** 2009 Stable expression and characterization of N-terminal tagged recombinant human bone morphogenetic protein 15. Mol Hum Reprod 15:779–788
18. **Moore RK, Otsuka F, Shimasaki S** 2003 Molecular basis of bone morphogenetic protein-15 signaling in granulosa cells. J Biol Chem 278:304–310
19. **Mishina Y, Suzuki A, Ueno N, Behringer RR** 1995 Bmpr encodes a type I bone morphogenetic protein receptor that is essential for gastrulation during mouse embryogenesis. Genes Dev 9:3027–3037
20. **Jamin SP, Arango NA, Mishina Y, Hanks MC, Behringer RR** 2002 Requirement of Bmpr1a for Müllerian duct regression during male sexual development. Nat Genet 32:408–410

21. **Mishina Y, Hanks MC, Miura S, Tallquist MD, Behringer RR** 2002 Generation of Bmpr/Alk3 conditional knockout mice. Genesis 32:69–72
22. **Soriano P** 1999 Generalized lacZ expression with the ROSA26 Cre reporter strain. Nat Genet 21:70–71
23. **Jeyasuria P, Ikeda Y, Jamin SP, Zhao L, De Rooij DG, Themmen AP, Behringer RR, Parker KL** 2004 Cell-specific knockout of steroidogenic factor 1 reveals its essential roles in gonadal function. Mol Endocrinol 18:1610–1619
24. **Jorgez CJ, Klysik M, Jamin SP, Behringer RR, Matzuk MM** 2004 Granulosa cell-specific inactivation of follistatin causes female fertility defects. Mol Endocrinol 18:953–967
25. **Fan HY, Liu Z, Paquet M, Wang J, Lydon JP, DeMayo FJ, Richards JS** 2009 Cell type-specific targeted mutations of Kras and Pten document proliferation arrest in granulosa cells versus oncogenic insult to ovarian surface epithelial cells. Cancer Res 69:6463–6472
26. **Petit FG, Jamin SP, Kurihara I, Behringer RR, DeMayo FJ, Tsai MJ, Tsai SY** 2007 Deletion of the orphan nuclear receptor COUP-TFII in uterus leads to placental deficiency. Proc Natl Acad Sci USA 104:6293–6298
27. **Lee KY, Jeong JW, Wang J, Ma L, Martin JF, Tsai SY, Lydon JP, DeMayo FJ** 2007 Bmp2 is critical for the murine uterine decidual response. Mol Cell Biol 27:5468–5478
28. **Erickson GF, Fuqua L, Shimasaki S** 2004 Analysis of spatial and temporal expression patterns of bone morphogenetic protein family members in the rat uterus over the estrous cycle. J Endocrinol 182: 203–217
29. **Finn CA, Martin L** 1972 Temporary interruption of the morphogenesis of deciduomata in the mouse uterus by actinomycin D. J Reprod Fertil 31:353–358
30. **Fan HY, Shimada M, Liu Z, Cahill N, Noma N, Wu Y, Gossen J, Richards JS** 2008 Selective expression of KrasG12D in granulosa cells of the mouse ovary causes defects in follicle development and ovulation. Development 135:2127–2137
31. **Kumar TR, Wang Y, Lu N, Matzuk MM** 1997 Follicle stimulating hormone is required for ovarian follicle maturation but not male fertility. Nat Genet 15:201–204
32. **Ma X, Dong Y, Matzuk MM, Kumar TR** 2004 Targeted disruption of luteinizing hormone β-subunit leads to hypogonadism, defects in gonadal steroidogenesis, and infertility. Proc Natl Acad Sci USA 101:17294–17299
33. **Shimasaki S, Zachow RJ, Li D, Kim H, Iemura S, Ueno N, Sampath K, Chang RJ, Erickson GF** 1999 A functional bone morphogenetic protein system in the ovary. Proc Natl Acad Sci USA 96:7282–7287
34. **ten Dijke P, Yamashita H, Sampath TK, Reddi AH, Estevez M, Riddle DL, Ichijo H, Heldin CH, Miyazono K** 1994 Identification of type I receptors for osteogenic protein-1 and bone morphogenetic protein-4. J Biol Chem 269:16985–16988
35. **Lavery K, Swain P, Falb D, Alaoui-Ismaili MH** 2008 BMP-2/4 and BMP-6/7 differentially utilize cell surface receptors to induce osteoblastic differentiation of human bone marrow-derived mesenchymal stem cells. J Biol Chem 283:20948–20958
36. **Yu PB, Beppu H, Kawai N, Li E, Bloch KD** 2005 Bone morphogenetic protein (BMP) type II receptor deletion reveals BMP ligand-specific gain of signaling in pulmonary artery smooth muscle cells. J Biol Chem 280:24443–24450
37. **Sicinski P, Donaher JL, Geng Y, Parker SB, Gardner H, Park MY, Robker RL, Richards JS, McGinnis LK, Biggers JD, Eppig JJ, Bronson RT, Elledge SJ, Weinberg RA** 1996 Cyclin D2 is an FSH-responsive gene involved in gonadal cell proliferation and oncogenesis. Nature 384:470–474
38. **Dunkel L, Tilly JL, Shikone T, Nishimori K, Hsueh AJ** 1994 Follicle-stimulating hormone receptor expression in the rat ovary: increases during prepubertal development and regulation by the opposing actions of transforming growth factors β and α. Biol Reprod 50:940–948
39. **Inoue K, Nakamura K, Abe K, Hirakawa T, Tsuchiya M, Oomori Y, Matsuda H, Miyamoto K, Minegishi T** 2003 Mechanisms of action of transforming growth factor β on the expression of follicle-stimulating hormone receptor messenger ribonucleic acid levels in rat granulosa cells. Biol Reprod 69:1238–1244
40. **Duman-Scheel M, Weng L, Xin S, Du W** 2002 Hedgehog regulates cell growth and proliferation by inducing cyclin D and cyclin E. Nature 417:299–304.
41. **Dennler S, André J, Alexaki I, Li A, Magnaldo T, ten Dijke P, Wang XJ, Verrecchia F, Mauviel A** 2007 Induction of sonic hedgehog mediators by transforming growth factor-β: Smad3-dependent activation of Gli2 and Gli1 expression in vitro and in vivo. Cancer Res 67:6981–6986
42. **Nolan-Stevaux O, Lau J, Truitt ML, Chu GC, Hebrok M, Fernandez-Zapico ME, Hanahan D** 2009 GLI1 is regulated through Smoothened-independent mechanisms in neoplastic pancreatic ducts and mediates PDAC cell survival and transformation. Genes Dev 23:24–36
43. **Livak KJ, Schmittgen TD** 2001 Analysis of relative gene expression data using real-time quantitative PCR and the $2^{-\Delta\Delta C_T}$ method. Methods 25:402–408
44. **Durlinger AL, Kramer P, Karels B, de Jong FH, Uilenbroek JT, Grootegoed JA, Themmen AP** 1999 Control of primordial follicle recruitment by anti-Mullerian hormone in the mouse ovary. Endocrinology 140:5789–5796
45. **Orvis GD, Jamin SP, Kwan KM, Mishina Y, Kaartinen VM, Huang S, Roberts AB, Umans L, Huylebroeck D, Zwijsen A, Wang D, Martin JF, Behringer RR** 2008 Functional redundancy of TGF-β family type I receptors and receptor-Smads in mediating anti-Mullerian hormone-induced Müllerian duct regression in the mouse. Biol Reprod 78:994–1001
46. **Mizunuma H, Liu X, Andoh K, Abe Y, Kobayashi J, Yamada K, Yokota H, Ibuki Y, Hasegawa Y** 1999 Activin from secondary follicles causes small preantral follicles to remain dormant at the resting stage. Endocrinology 140:37–42
47. **Yokota H, Yamada K, Liu X, Kobayashi J, Abe Y, Mizunuma H, Ibuki Y** 1997 Paradoxical action of activin A on folliculogenesis in immature and adult mice. Endocrinology 138:4572–4576
48. **Pangas SA, Jorgez CJ, Tran M, Agno J, Li X, Brown CW, Kumar TR, Matzuk MM** 2007 Intraovarian activins are required for female fertility. Mol Endocrinol 21:2458–2471
49. **Yan C, Wang P, DeMayo J, DeMayo FJ, Elvin JA, Carino C, Prasad SV, Skinner SS, Dunbar BS, Dube JL, Celeste AJ, Matzuk MM** 2001 Synergistic roles of bone morphogenetic protein 15 and growth differentiation factor 9 in ovarian function. Mol Endocrinol 15: 854–866
50. **McMullen ML, Cho BN, Yates CJ, Mayo KE** 2001 Gonadal pathologies in transgenic mice expressing the rat inhibin α-subunit. Endocrinology 142:5005–5014
51. **Lan ZJ, Gu P, Xu X, Jackson KJ, DeMayo FJ, O'Malley BW, Cooney AJ** 2003 GCNF-dependent repression of BMP-15 and GDF-9 mediates gamete regulation of female fertility. EMBO J 22:4070–4081
52. **Williams SA, Stanley P** 2008 Mouse fertility is enhanced by oocyte-specific loss of core 1-derived *O*-glycans. FASEB J 22:2273–2284
53. **Ebisawa T, Tada K, Kitajima I, Tojo K, Sampath TK, Kawabata M, Miyazono K, Imamura T** 1999 Characterization of bone morphogenetic protein-6 signaling pathways in osteoblast differentiation. J Cell Sci 112(Pt 20):3519–3527
54. **Macías-Silva M, Hoodless PA, Tang SJ, Buchwald M, Wrana JL** 1998 Specific activation of Smad1 signaling pathways by the BMP7 type I receptor, ALK2. J Biol Chem 273:25628–25636
55. **Guo X, Wang XF** 2009 Signaling cross-talk between TGF-β/BMP and other pathways. Cell Res 19:71–88
56. **Matzuk MM, Finegold MJ, Su JG, Hsueh AJ, Bradley A** 1992 α-Inhibin is a tumour-suppressor gene with gonadal specificity in mice. Nature 360:313–319
57. **Matzuk MM, Finegold MJ, Mather JP, Krummen L, Lu H, Bradley A** 1994 Development of cancer cachexia-like syndrome and adrenal tumors in inhibin-deficient mice. Proc Natl Acad Sci USA 91:8817–8821
58. **Li Q, Graff JM, O'Connor AE, Loveland KL, Matzuk MM** 2007

SMAD3 regulates gonadal tumorigenesis. Mol Endocrinol 21:2472–2486

59. **Li Q, Kumar R, Underwood K, O'Connor AE, Loveland KL, Seehra JS, Matzuk MM** 2007 Prevention of cachexia-like syndrome development and reduction of tumor progression in inhibin-deficient mice following administration of a chimeric activin receptor type II-murine Fc protein. Mol Hum Reprod 13:675–683
60. **Sharov AA, Mardaryev AN, Sharova TY, Grachtchouk M, Atoyan R, Byers HR, Seykora JT, Overbeek P, Dlugosz A, Botchkarev VA** 2009 Bone morphogenetic protein antagonist noggin promotes skin tumorigenesis via stimulation of the Wnt and Shh signaling pathways. Am J Pathol 175:1303–1314
61. **Rubin LL, de Sauvage FJ** 2006 Targeting the hedgehog pathway in cancer. Nat Rev 5:1026–1033
62. **Liao X, Siu MK, Au CW, Wong ES, Chan HY, Ip PP, Ngan HY, Cheung AN** 2009 Aberrant activation of hedgehog signaling pathway in ovarian cancers: effect on prognosis, cell invasion and differentiation. Carcinogenesis 30:131–140
63. **Wijgerde M, Ooms M, Hoogerbrugge JW, Grootegoed JA** 2005 Hedgehog signaling in mouse ovary: Indian hedgehog and desert hedgehog from granulosa cells induce target gene expression in developing theca cells. Endocrinology 146:3558–3566
64. **Russell MC, Cowan RG, Harman RM, Walker AL, Quirk SM** 2007 The hedgehog signaling pathway in the mouse ovary. Biol Reprod 77:226–236
65. **Howe JR, Bair JL, Sayed MG, Anderson ME, Mitros FA, Petersen GM, Velculescu VE, Traverso G, Vogelstein B** 2001 Germline mutations of the gene encoding bone morphogenetic protein receptor 1A in juvenile polyposis. Nat Genet 28:184–187
66. **Waite KA, Eng C** 2003 From developmental disorder to heritable cancer: it's all in the BMP/TGF-β family. Nat Rev Genet 4:763–773
67. **Lee J, Son MJ, Woolard K, Donin NM, Li A, Cheng CH, Kotliarova S, Kotliarov Y, Walling J, Ahn S, Kim M, Totonchy M, Cusack T, Ene C, Ma H, Su Q, Zenklusen JC, Zhang W, Maric D, Fine HA** 2008 Epigenetic-mediated dysfunction of the bone morphogenetic protein pathway inhibits differentiation of glioblastoma-initiating cells. Cancer Cell 13:69–80
68. **Yi SE, Daluiski A, Pederson R, Rosen V, Lyons KM** 2000 The type I BMP receptor BMPRIB is required for chondrogenesis in the mouse limb. Development 127:621–630
69. **Edson MA, Lin YN, Matzuk MM** 2010 Deletion of the novel oocyte-enriched gene, Gpr149, leads to increased fertility in mice. Endocrinology 151:358–368
70. **Nagaraja AK, Andreu-Vieyra C, Franco HL, Ma L, Chen R, Han DY, Zhu H, Agno JE, Gunaratne PH, DeMayo FJ, Matzuk MM** 2008 Deletion of Dicer in somatic cells of the female reproductive tract causes sterility. Mol Endocrinol 22:2336–2352